TESTING AND CHARACTERIZATION OF WAVY COMPOSITES

Dr. William F. Pratt and Matthew S. Allen
Patterned Fiber Composites, Inc.
Lindon, UT 84042

Dr. Scott D. Sommerfeldt
Brigham Young University
Provo, UT 84602

ABSTRACT

Wavy composite is a new form of constrained layer damping that uses opposing sinusoidal waveforms and viscoelastic materials to provide both high damping *and* stiffness. This article discusses one method of testing wavy composites that determines the stiffness and damping of the material over a broad band of frequencies and temperatures. These material properties can then be used to design practical structures using a design-of-experiments, or can be used to validate the material model in a finite element analysis (FEA) program. Test results are used to characterize the material properties of wavy composites and correlate the results to a FEA model developed by Patterned Fiber Composites, Inc. Test data collected over an extended temperature range is combined using the WLF equation, to create a "master" damping and modulus vs frequency curve for a single temperature over a broad frequency range. Generally known as "nomographs" these charts can provide the designer with a flexible design tool that relates temperature, frequency, and performance of the wavy composite lay-up. Damping measurements as high as 30% with the stiffness of aluminum and titanium using standard graphite fibers are reported.

KEY WORDS: Advanced Composites, Carbon Fiber, Characterization, Composite Materials, Testing/Evaluation, Viscoelasticity

1. INTRODUCTION

Wavy composite is a new, and emerging form of constrained layer damping that uses standard fibers, resins, and viscoelastic materials in a new configuration to provide both high damping *and* stiffness. Originally conceived in 1990 by Dr. Benjamin Dolgin of NASA (Dolgin 1990), a practical way of implementing this concept did not exist until 1997 (Pratt 1999). During the period from 1997 to mid 2000 advances in FEA modeling and prediction, material selection, and testing led to a number of important discoveries. Dolgin's concept is shown in Figure 1.

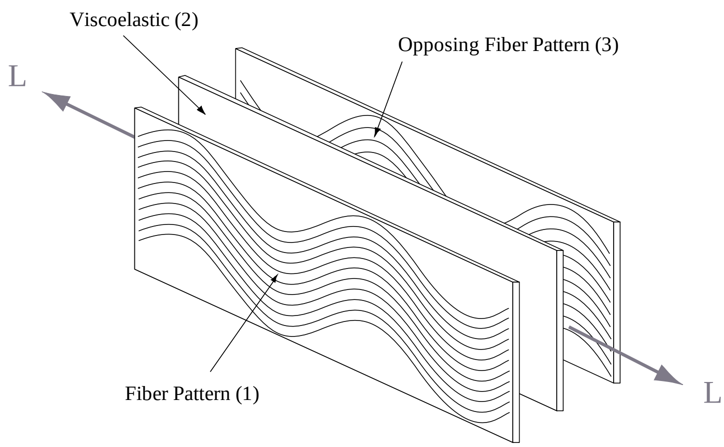

Figure 1: Basic damped wavy composite concept

The viscoelastic layer dominates damping and stiffness performance of a wavy composite combination. As a result, all the concepts that apply for a linear viscoelastic material apply to the combination of wavy composite and viscoelastic material, namely (Pratt, et al. 2001):

1. Wavy composites exhibit glass transitional properties, i.e. there are defined asymptotic values for stiffness, and a defined damping peak as a function of temperature and frequency.
2. Frequency-temperature superposition, i.e. a change in temperature is equivalent to a change in frequency.
3. Viscoelasticity, i.e. damping can be approximated by factoring the modulus or stiffness of a material.

Unlike more conventional methods of material testing of fiber reinforced plastics, methods used to test wavy composite structures must account for the frequency and temperature dependence of the viscoelastic materials used in the structure. While the damping and stiffness properties of the composites used in the constraining layers are essentially independent of temperature and frequency (Gibson 1976), this is not true of viscoelastic materials. Thus, meaningful characterization of these material combinations can only be accomplished with a dynamic test.

The method explained in this paper determines the complex material properties related to modulus and damping in a linearly viscoelastic structural material as a function of time and frequency. This method effectively decouples the dynamic resonance of the test specimen by using a mathematical model of the specimen and curve-fitting each data point to the model by iteration. The result provides a complex modulus for the material used in the fabrication of the specimen that can be used to evaluate the results of FEA models, predict performance in other structures, and create a “master nomograph” of the material for design purposes.

2. TEST CONCEPT

The test method is based on a concept proposed in the testing of viscoelastic samples (Nielsen, et al. 2000). Since wavy composites are considerably stiffer than viscoelastic materials, several modifications and improvements were accomplished which provided accurate results.

Nielsen et al used an accelerometer and a load cell to measure axial displacement and force applied to the driven end of their sample. They assumed displacement at the stationary end would be exactly zero or small enough as to be insignificant (Nielsen, et al. 2000). Because the sample stiffness was insignificant relative to the base structure, their assumption was reasonable and simplified the analysis. Such is not the case with a stiffer material.

Since wavy composites exhibit both high damping and stiffness, the dynamics of the test structure cannot be ignored but their effects were minimized and the results proved to be more accurate. Instead of using an accelerometer and load cell on the driven end of the sample and driving it against an immovable base as Nielsen used, the method presented here used two accelerometers, one at each end, driving the sample in a fixed-free mode. The test setup is shown below.

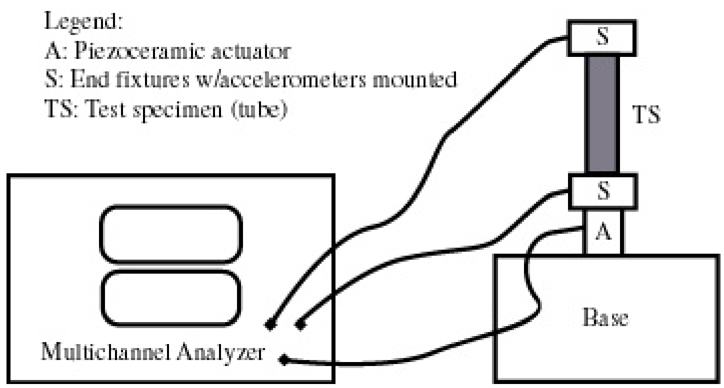

Figure 2: Test setup

The wavy composite test tube was mounted between two test fixtures, which also provided a mount for the accelerometers. The tube was driven axially by a piezoceramic actuator driven by an amplifier using white noise. Since the mass of the end fixtures, and the mass and the dimensions of the tube can be accurately measured, the only unknowns are the stiffness and damping, and as will be shown, these can be determined from the transfer function of the two accelerometers with good accuracy.

3. ALGORITHM

Axial excitation of the test specimen was chosen because the material properties can be determined directly. Since the structure of the tube is composed of two or more dissimilar materials (in this case wavy composite and viscoelastic), the material properties derived represent the average or “smear” properties. If it is assumed that the primary load resistance is provided by the composite constraining layers, the equivalent material properties of the composite can be determined by factoring the sample by the area of the composite. This provides a relative measure of the stiffness of an equivalent “composite only” sample. Because the test method is robust enough to measure a stiff structural material it is also capable of determining the properties of conventional composites without viscoelastic layers. This provided a very convenient method of testing and verifying the composite constants used in finite element analysis.

The model of the tube-test setup used to determine the material properties of a given sample is derived from the solution to the partial differential equation (and boundary condition (BC)) for longitudinal vibrations shown in Equation one:

$$\frac{\partial^2 u}{\partial x^2} - \frac{1}{c^2}\frac{\partial^2 u}{\partial t^2} = f(t) \quad \textit{subject to BC}: \quad EA\frac{\partial u}{\partial x}(L,t) = -m\frac{\partial^2 u}{\partial t^2}(L,t) \qquad \text{Eqn. 1}$$

Where "c" is the speed of sound in the material, and c and ω are defined as follows:

$$c = \sqrt{\frac{E^*}{\rho}} \quad and \quad \omega = \lambda c \qquad \text{Eqn. 2}$$

The solution to Equation one is given by the following:

$$U(x,t) = X(t)T(t) \qquad \text{Eqn. 3}$$

$$X(x) = c_1 \cos\lambda x + c_2 \sin\lambda x \qquad \text{Eqn. 4}$$

$$T(t) = c_3 \cos\lambda ct + c_4 \sin\lambda ct \qquad \text{Eqn. 5}$$

Applying the simplified versions of Equations 4 & 5 to Equation 1 gives the following:

$$EA \cdot X'T = m\lambda^2 c^2 \cdot XT \quad or \quad EA \cdot X'(L) = m\lambda^2 c^2 \cdot X(L) \qquad \text{Eqn. 6}$$

The use of Equation 5 is no longer needed and combination of Equations 4 & 6 results in the determination of the ratio of the c_1 and c_2 constants:

$$\frac{c_2}{c_1} = \frac{m\omega^2 \cos\lambda L + EA\lambda \sin\lambda L}{EA\lambda\cos\lambda L - m\omega^2 \sin\lambda L} \qquad \text{Eqn. 7}$$

The "compliance" version of the transfer function for the two accelerometers is:

$$\frac{U(L,t)}{U(0,t)} = \frac{c_1 \cos\lambda L + c_2 \sin\lambda L}{c_1} = \cos\lambda L + \frac{c_2}{c_1}\sin\lambda L \qquad \text{Eqn. 8}$$

Substituting Equation 7 into Equation 8 and inverting the result gives:

$$\frac{U(0,t)}{U(L,t)} = \cos\beta - \frac{Mass_L}{Mass_{tube}}\beta\sin\beta \qquad \text{Eqn. 9}$$

Where the mass at the free end ($Mass_L$) is m in Equation 7, and the mass of the tube is the product of the density, cross sectional area, and the length of the tube. β is a function of the length L, the frequency, the density of the test specimen, and the complex modulus E^*:

$$\beta = \sqrt{\frac{L^2\omega^2\rho}{E^*}} \qquad \text{Eqn. 10}$$

By applying Equations 9 and 10 to the transfer data at each measurement frequency, iterative solutions will converge on a β (and therefor a complex modulus E^*) that will satisfy the Equations. The method converges rapidly using Newton's method where:

$$y = \frac{U(0,t)}{U(L,t)} - \cos\beta + \frac{Mass_L}{Mass_{tube}}\beta\sin\beta \qquad \text{Eqn. 11}$$

$$\frac{\partial y}{\partial \beta} = \sin\beta + \frac{Mass_L}{Mass_{tube}} \sin\beta + \frac{Mass_L}{Mass_{tube}} \beta \cos\beta \qquad \text{Eqn. 12}$$

$$\beta_{i+1} = \beta_i - \frac{y}{\dfrac{\partial y}{\partial \beta}} \qquad \text{Eqn. 13}$$

The ratio shown in the second term of Equation 13 represents the "delta β" and is driven towards zero as the β converges on a solution, once an initial guess is made for the complex modulus E^*. Equations 10 through 13 are placed in a while loop and solved in the order shown until the absolute value of "delta β" is below an acceptable value. The complex modulus is then solved using an appropriate form of Equation 10. This occurs for each frequency measurement of the transfer function. The result is a table or plot of the real component of the modulus and the damping constant given in the following:

$$E^* = E' + E'' = E + j\eta E = E \cdot (1 + j\eta) \qquad \text{Eqn. 14}$$

Internal studies have shown that the method is quite robust and is very forgiving of initial guesses that are off by as much as 50% or more on both damping and modulus. Convergence is rapid and the whole process takes less time to solve and plot than it takes to obtain the data.

4. IMPROVING PERFORMANCE

This method works best for structural materials over a frequency range centered on the first axial resonance. Considerable error can occur if the frequency range is extended too far from the first axial resonance and appears to be associated with a number of causes including spurious resonance associated with the structure (e.g. not associated with the test sample), sensor noise, and phase angle measurement error or noise. Error associated with the test structure was eliminated by attaching the actuator, end fixtures, and accelerometers to a solid cylindrical chunk of steel. The entire structure was then isolated from the building dynamics by laying it on a half-inch sheet of vibration damping material. Other spurious structural modes derived from bending of the tubes. These errors were eliminated by co-axially mounting the accelerometers with the centerline of the tube.

Sensor noise was the biggest contributor to error in the measurements of magnitude and phase once these other problems were solved. Some of the sensor noise was caused by electrical noise transmitted through the body of the specimen to the accelerometers. This was easily resolved by electrically isolating the accelerometers from any conductive surfaces of the tube or end mounts.

The remaining sensor noise was associated with the sensitivity floors of the accelerometers, especially at frequencies removed from the primary resonance. This is due primarily to two causes. First, not enough energy is applied to the structure at low frequencies. With a conventional white noise generator, the energy imparted to the structure is spread across the frequency spectrum. The accelerometer measures acceleration and is therefore proportional to $x\omega^2$. At frequencies well below the first resonate mode, the force imparted to the structure is too low to measure accurately.

Secondly, at anti-resonance and frequencies well away from resonance modes (especially for low damped composites) phase angles are very close to zero. This means that the natural noise floor for the sensor can be greater than the value of the phase angle being measured. This is less problematic for tubes with greater damping. Even so, undamped tubes of conventional unidirectional composite have been successfully tested and have shown to exhibit both modulus and damping accurately. In fact, testing of 90° unidirectional composite tubes (used to determine the E22, E33 modulus) produce more believable results than the standard ASTM methods, *and* the tube samples are easier to make.

5. TYPICAL RESULTS

The following shows the typical test results of tubes made with wavy composite. The analysis shown below was obtained from a tube made using wavy material with a 7.6 cm wave period and 25 degree max angle. Results from 0 to 3200 hertz are shown but as can be seen in Figure 3, noise in the measurement below 400 hertz made the data meaningless.

The method used to analyze this and other tubes decouples the mass from the system and allows accurate measurement of damping and stiffness over a frequency band of .2 f_r to 2 f_r. The main source of error in determining damping and stiffness stems from noise in the measurement of magnitude and phase angle at frequencies lower than about .3 f_r or above 3 f_r where the phase angle is close to 0° or 180°.

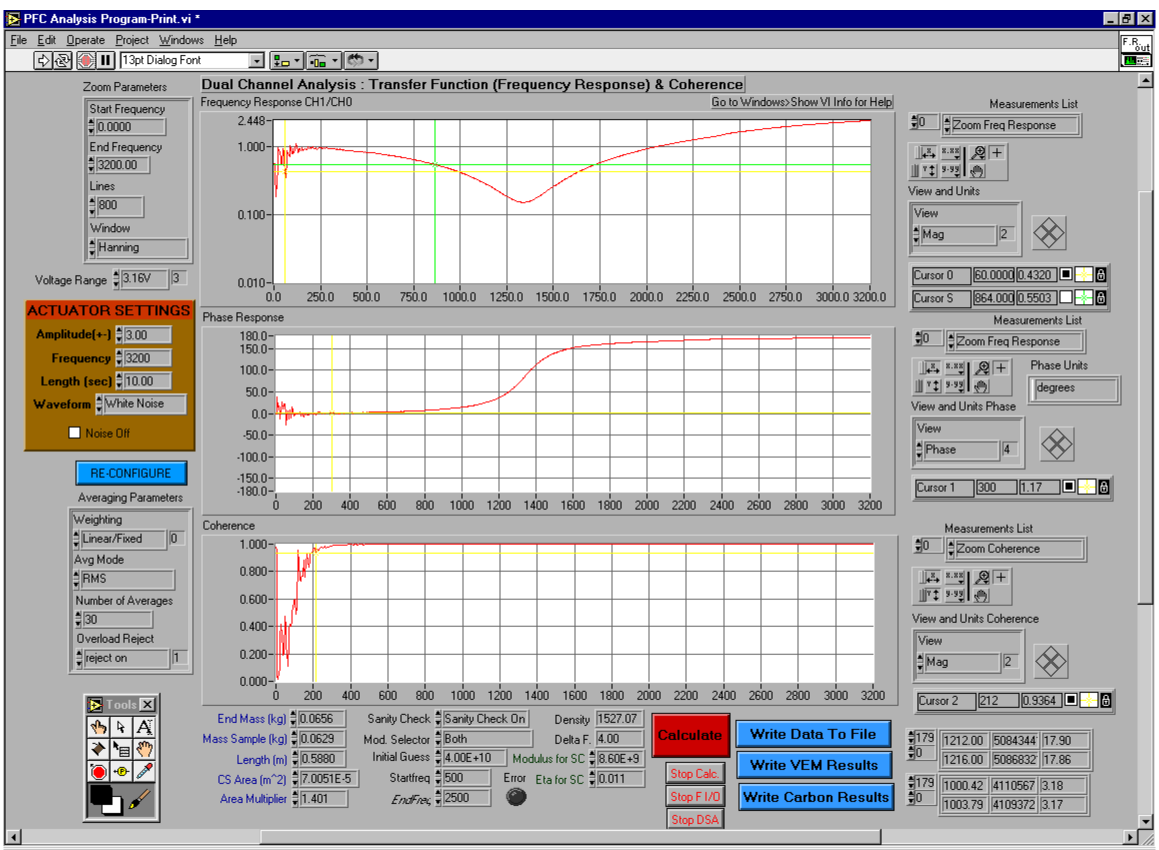

Figure 3: Magnitude, phase, and coherence plots for a wavy composite tube at 50°C

As shown in Figure 3, the magnitude drops off (probably due to insufficient activation) and noise in the phase angle becomes pronounced between 0 and 250 hertz. This is reflected in the measurement of coherence shown in Figure 3. As shown, coherence is at or close to 100% for frequencies between 400 and 3200 hertz. Below 400 hertz the coherence begins to drop off until at 250 hertz, the coherence measurement is so low that the data becomes meaningless.

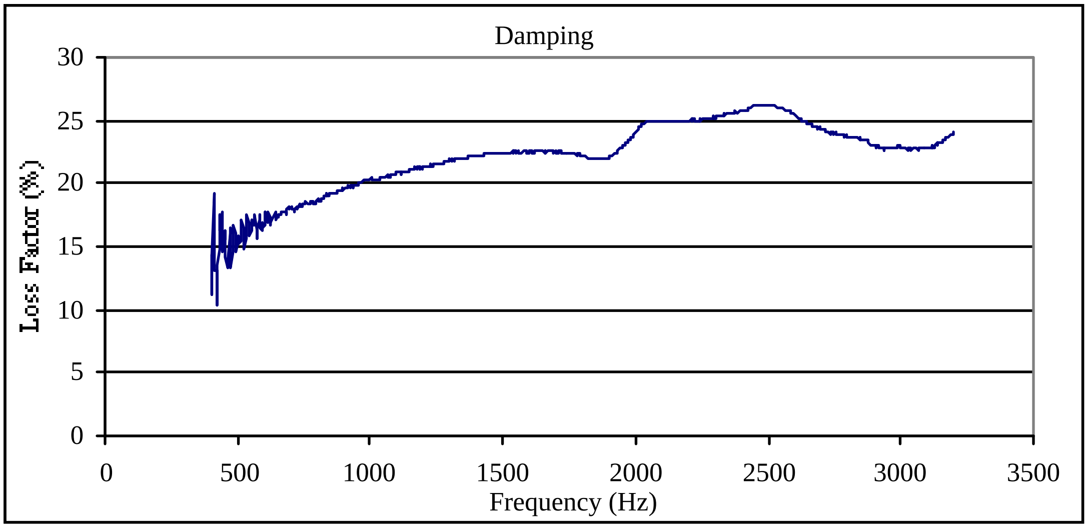

Figure 4: Axial damping results plot for a wavy composite tube at 50°C

Using the algorithm discussed above, the damping and stiffness for the tube over the range of 400 to 3200 hertz can be determined. Figure 4 shows the decoupled damping results calculated from the magnitude and phase information shown in Figure 3. The results show that noise trends in the damping strongly mirror the noise in the measurement of phase angle as would be expected. Despite the noise, the low frequency trend in damping is still very much apparent, starting at 16% and moving generally upward toward a peak of 26% at about 2500 Hz.

Stiffness prediction does not seem to be as sensitive to noise in the measurement of magnitude or phase angle. Figure 5 shows a relatively clean stiffness prediction between 400 and 3200 hertz. As expected for a material with viscoelastic properties, the stiffness increases steadily from about 30 GPa to a peak of 39 GPa at 3200 hertz. The term stiffness is used here to represent a "smeared" property over the thickness of the tube and includes the viscoelastic layer.

Figures 4 and 5 show the damping and stiffness results for a tube at a single temperature. If data for the same test specimen is collected over an extended temperature range, the results of each test can be combined using the WLF equation, to create a "master" damping and modulus versus frequency curve for a reference temperature over a broad frequency range. Generally known as "nomographs" these charts can provide the designer with a flexible design tool that relates temperature, frequency, and performance of the wavy composite lay-up.

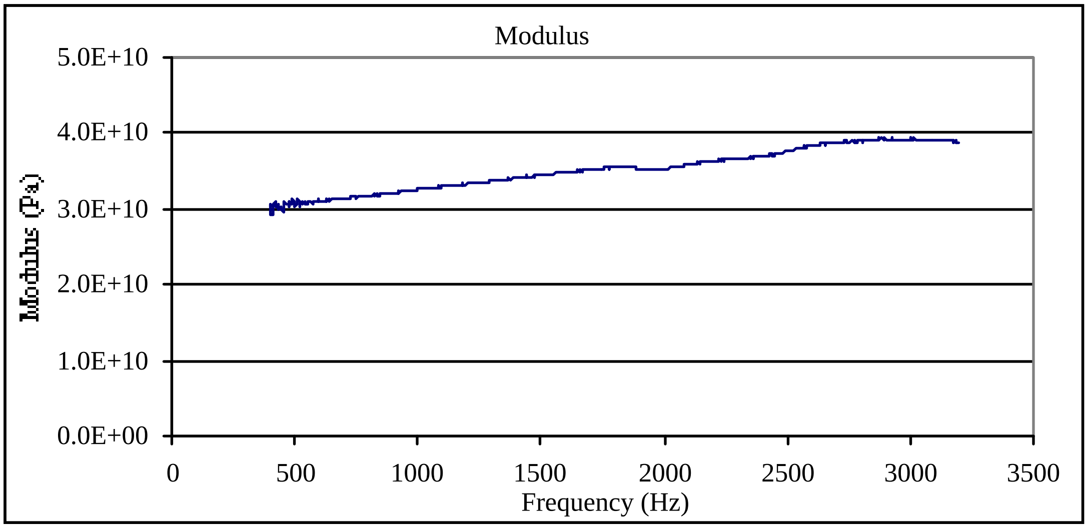

Figure 5: Stiffness results plot for a wavy composite tube at 50°C

6. WAVY COMPOSITE NOMOGRAPHS, TIME TEMPERATURE SUPERPOSITION AND WLF

The noise in the stiffness and damping results limit the range of reliable test data to approximately 500-2500 Hz. Therefore, without using a different experimental setup it is impossible to collect low frequency data directly with this test equipment. However, it is not difficult to collect data over the 500-2500 Hz frequency range at a wide range of temperatures. Figure 6 shows the experimentally measured stiffness of a composite tube from 500-2000 Hz at a number of temperatures.

Figure 6 shows the effects of temperature or frequency. Note that increasing the temperature of the composite tube lowers the stiffness curve over the testable freqency range. Also note that the stiffness generally increases with increasing frequency. This behavior agrees with the expected performance of a viscoelastic material. The time-temperature superposition principle states that a material will behave predictably to changes in temperature or frequency. Increasing temperature is identical to decreasing frequency and visa versa. The curves in Figure 6 represent the performance of the material over the same *frequency* range but different temperatures. If the results are normalized for the same *temperature*, the result will be to shift the frequency of each curve by an amount determined by the WLF equation.

Equation 15 describes this behavior mathematically, where f_2 is a shifted frequency, f_1 is the original frequency and $\alpha(T)$ is a shift factor. The shift factor is a function of temperature, and quantifies the relationship between frequency and temperature for the given material.

$$f_2 = f_1(\alpha(T)) \qquad \text{Eqn. 15}$$

A good equation for $\alpha(T)$ is the William Landel Ferry Equation 16. This equation has been shown to have universal application over a wide variety of polymer materials (Ferry 1980).

$$\log[\alpha(T)] = \frac{-c_1(T-T_0)}{c_2+T-T_0} \quad \textbf{(WLF equation)} \qquad \text{Eqn. 16}$$

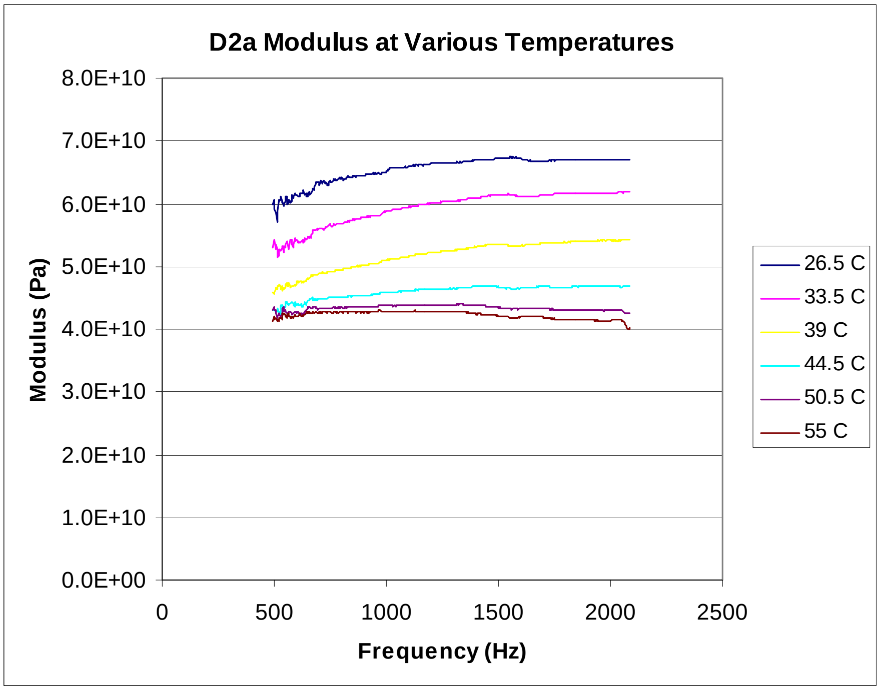

Figure 6: Measured elastic modulus of composite tube at various temperatures (500-2000 Hz).

If Equation 16 is substituted into Equation 15, the result is Equation 17. In this equation the shifted frequency is replaced by "reduced frequency" FR, which takes temperature into account. Through the use of this equation, time temperature superposition can be used to construct a single master curve over a broad frequency range. The application of time-temperature superposition through the WLF equation will be discussed later.

$$\log(FR) = \log(F) - \frac{c_1(T - T_0)}{c_2 + T - T_0} \qquad \text{Eqn. 17}$$

Figure 7 shows the data from Figure 6 shifted to a reference temperature of 25° C where the x-axis represents a reduced frequency. (The following values were used in the WLF equation: c_1 = 12, c_2 = 160, T_0 = 25° C.)

If we let T= T_0 = 25° C, equation 17 reduces to F = FR. Thus Figure 7 also represents the dynamic performance of the composite tube at 25° C from 10 to 3000 Hz. Application of the time-temperature superposition principle has created the "master" modulus curve for the sample. The data have been shifted to produce a continuous line covering a larger range of frequency. This allows characterization of the sample for much lower or higher frequencies than is physically possible with test equipment by simply changing the temperature of the test specimein.

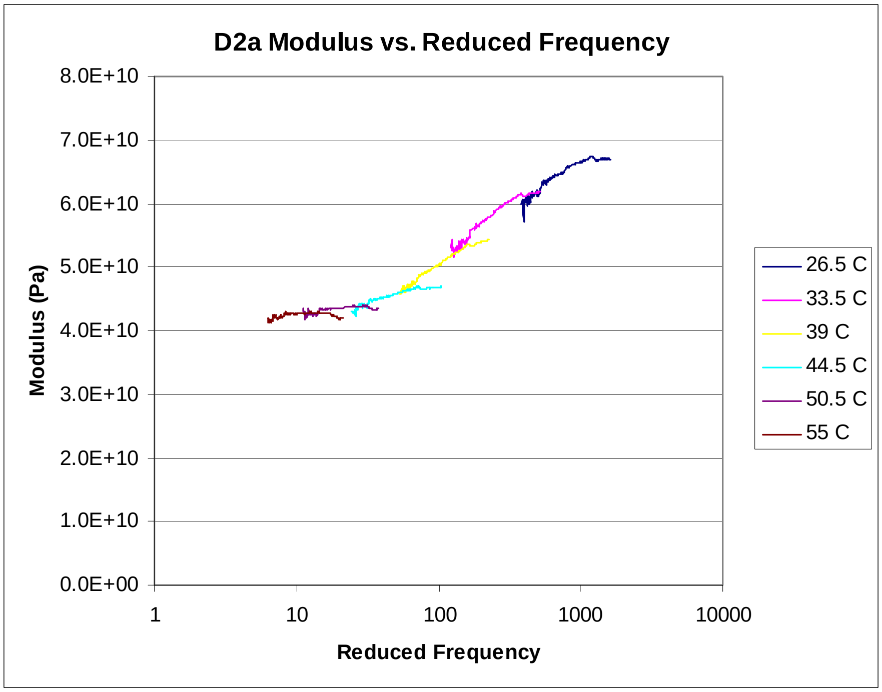

Figure 7: Modulus vs. Reduced Frequency referenced to 25° C

By changing the reference temperature (T_0) we can easily create a master curve of the data at any temperature. Given initial values for the WLF constants (T_0, c_1, c_2), new values for c_1 and c_2 can be found corresponding to new T_0 with the following equations (18, 19).

$$c_{1,new} = \frac{c_1 c_2}{c_2 + T_{0,new} - T_0} \qquad \text{Eqn. 18}$$

$$c_{2,new} = c_2 + T_{0,new} - T_0 \qquad \text{Eqn. 19}$$

Where $c_{1,\ new}$ and $c_{2,\ new}$ are the new c_1 and c_2 constants respectively and $T_{0,\ new}$ is the new reference temperature (Sperling 1989).

7. FREQUENCY TEMPERATURE NOMOGRAPHS

A convenient way of displaying the data is the frequency-temperature nomogram. Figure 8 shows the elastic modulus and damping of the same test data on a frequency temperature nomogram. This nomogram is also referenced to 25° C, thus at 25° C the actual frequency (in Hz) can be read directly on the "reduced frequency" scale.

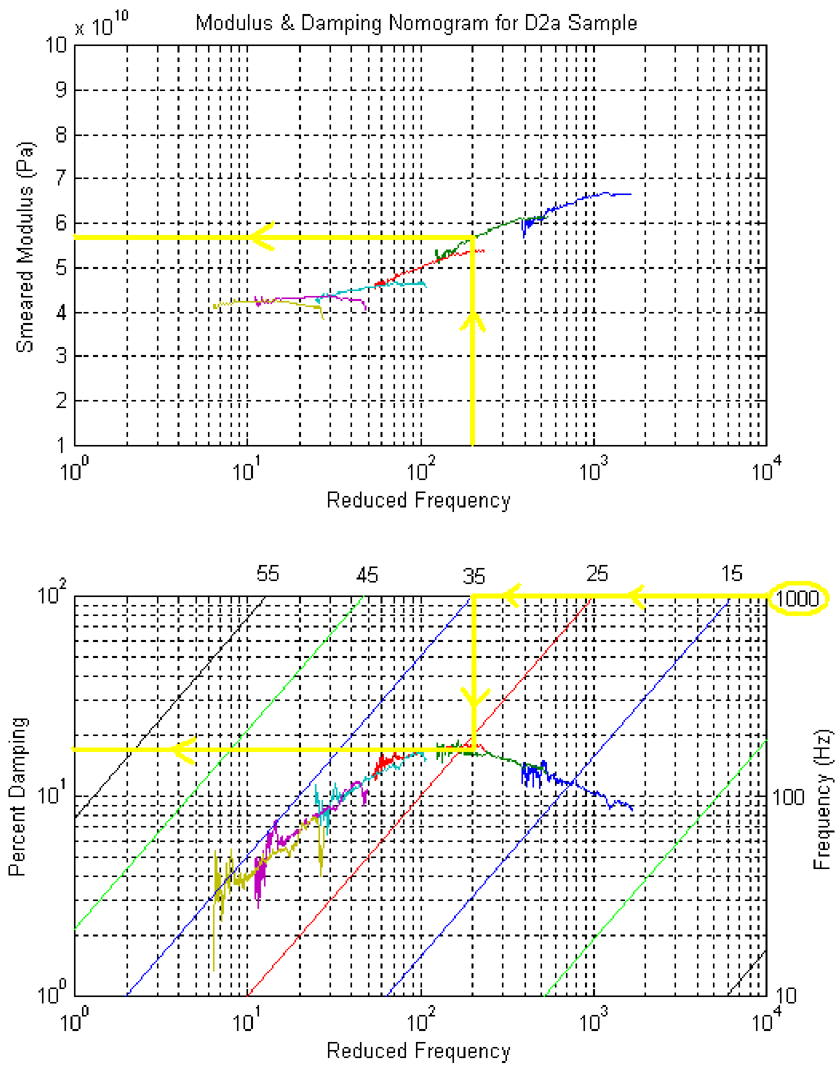

Figure 8: Modulus and Damping of D2a sample Frequency-Temperature Nomogram

For other temperatures the modulus and damping can be read by using the temperature lines. For example, if we wish to know the loss factor and damping at 1000 Hz and 35° C: First locate 1000 Hz on the far right "frequency (Hz)" axis. Follow this line to the left until reaching the diagonal temperature line labeled 35° C. (Note that the reduced freqency value at this point is approximately 200 Hz. Thus 1000 Hz at 35° C is equivalent to 200 Hz at 25° C). Now read up or down to the modulus or damping master curve. From this point the modulus or damping value can be read by traveling horizontally to the far left scale as illustrated by the thick lines. The values are approximately 57 Gpa for the elastic modulus and 18% damping.

8. WLF CONSTANT DETERMINATION

Rodger N. Capps and Linda L. Beumel describe a method for determining the WLF constants through a computer algorithym (Sperling 1989). The basic process will now be described in further detail, though automation will be left to the reader.

Figure 6 shows test data collected at various temperatures. For convenience the highest observed temperature is taken as the reference temperature (55° C in this case). The shift factor $\delta\alpha_t$ is defined as the ratio of shifted frequency to the reference frequency. For each set of data at distinct temperatures a shift factor is recorded. For example, note that the modulus has a value of 60 GPa at 546 Hz at 26.5° C and also at 1179 Hz and 33.5° C. Thus in order to shift the data at 26.5° C so that it lies on the curve at the next hightest temperature 33.5° C, it would have to be multiplied by the shift factor $\delta\alpha_t$ = (1179/546). The log of the shift factors is taken, and the $\log(\delta\alpha_t)$ are added beginning at the reference temperature (55° C) resulting in a value of the log shift factor $\log(\alpha_t)$ for each temperature tested. Table 1 shows sample data taken from Figure 6:

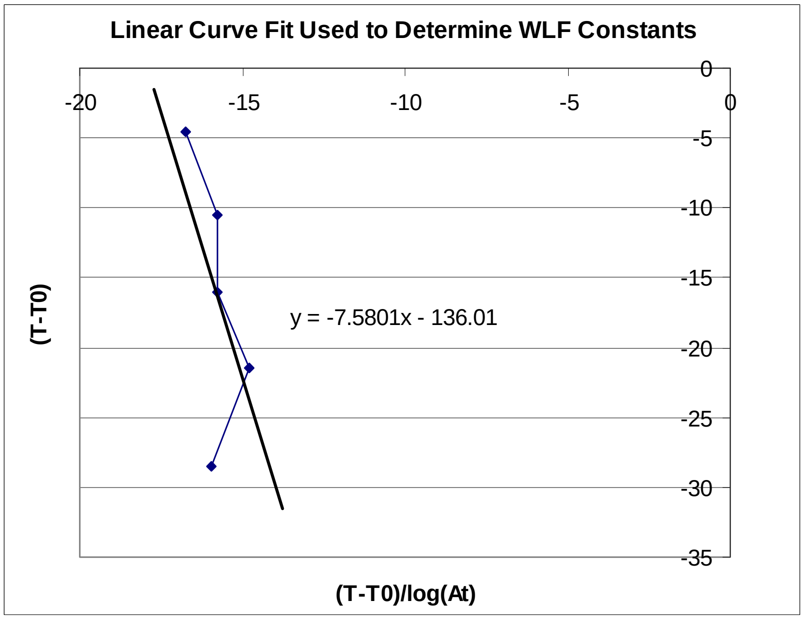

Figure 9: Linear curve fit used to determine WLF constants. (55° C Ref. Temperature)

Thus a linear curve fit between $(T-T_0)/\log(\alpha_t)$ and $(T-T_0)$ yields $-c_1$ as the slope and $-c_2$ as the intercept. Figure 9 illustrates this. Note that there was some scatter in data. This is probably due to human error in determining the amount of frequency shift required. It is also possible to fit a curve through each section of data and use an iterative technique to converge on the shift factor required to cause the sets of data to align. The constants can now be adjusted for any reference temperature through equations 18 and 19. Shifting the constants in Figure 9 to 25° C yields c_1 = 9.73 and c_2 = 106. Figure 10 shows the data from Figure 6 shifted with these new constants. The resultant smoothness of the damping plot is an independent verification that the constants are correct.

Table 1: WLF Constant Determination Data

Temperature	26.5	33.5	39	44.5	50.5	55
(T-T0)	-28.5	-21.5	-16	-10.5	-4.5	0
Shifted F	1179	1381	1070	1320	1300	
Ref. F	546	500	480	530	700	
delta At	2.15934	2.762	2.22917	2.49057	1.85714	1
log(delta At)	0.33432	0.44122	0.34814	0.3963	0.26885	0
log(At)	1.78883	1.45451	1.01329	0.66514	0.26885	0
At	61.4937	28.478	10.3106	4.62534	1.85714	1
(T-T0)/log(At)	-15.9322	-14.7816	-15.7902	-15.7861	-16.7382	

WLF equation (1) can be rearranged into the form shown in equation 20.

$$(T - T_0) = -c_1\left(\frac{(T - T_0)}{\log[\alpha(T)]}\right) - c_2 \qquad \text{Eqn. 20}$$

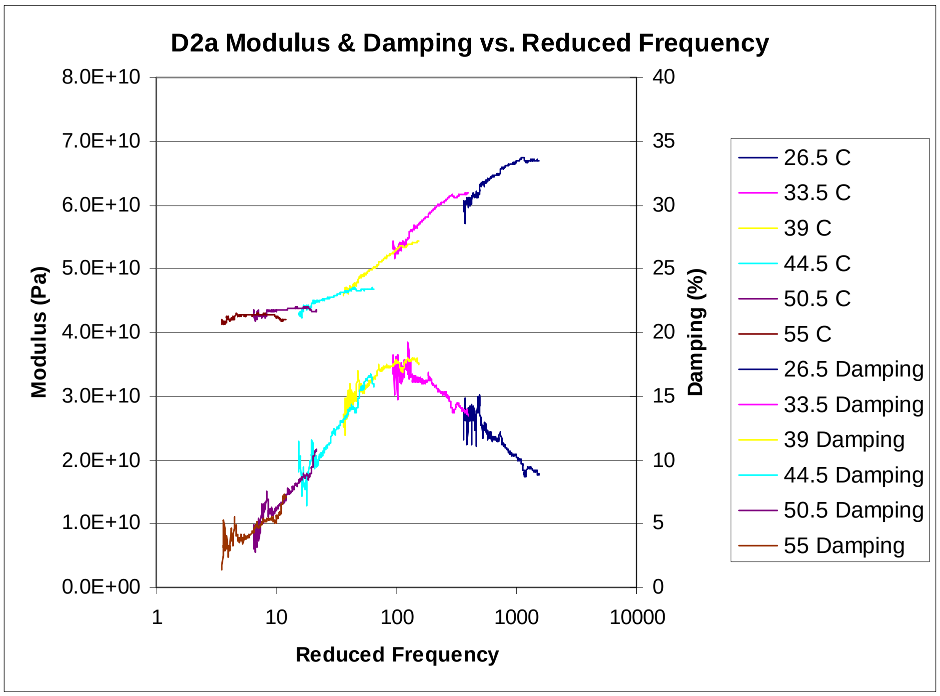

Figure 10: Shifted modulus & damping curves using c_1 = 9.73 and c_2 = 106, at 25° C

9. CONCLUSIONS

This paper has discussed and shown examples of how wavy composite tubes can be tested to determine damping and stiffness performance over a broad frequency band. By using the temperature-frequency superposition principle and the WLF equation, it is possible to create a "master curve" or nomograph of both damping and stiffness for a broader frequency band than can be physically tested. The method is robust, and cost effective to operate and provides a simple means by which highly damped structural materials such as wavy composites can be

tested. This work was supported by the Air Force Research Laboratory and their support is gratefully acknowledged.

10. REFERENCES

US Patent No. 5,203,435, (1990) B. P. Dolgin, (NASA).

W. F. Pratt, Patterned Fiber Composites, Process, Characterization, and Damping Performance, Ph.D. Dissertation, Brigham Young University, Provo, Utah, (1999).

W. F. Pratt, M. Allen and C. G. Jensen, “Designing with Wavy Composites,” SAMPE 2001, SAMPE, Long Beach, CA, (2001).

R. F. Gibson, Journal of Composite Materials, **10,** 325-341 (1976).

L. F. Nielsen, N. J. Wismer and S. Gade, “An Improved Method for Estimating the Dynamic Properties of Materials,” Journal of Sound and Vibration, 20-24, (2000).

J. D. Ferry, Viscoelastic Properties of Polymers, John Wiley & Sons, 1980, 672.

L. H. Sperling, Science and Engineering at the 197th National Meeting of the American Chemical Society, 5-22, (1989).